Flavobacteria buffer nitrous oxide emissions from partial denitrifiers in coastal sediments

Thanh Nguyen-Dinh[1*], Tess Hutchinson[1], Francesco Ricci[1], Hanif Prayitno[2], Luis Jimenez[1], Vera Eate[2], Pok Man Leung[1], Rachael Lappan[1], Sukhwan Yoon[3], Wei Wen Wong[2], Perran L.M. Cook[2], Chris Greening[1*]

[1]Department of Microbiology, Biomedicine Discovery Institute, Monash University, Clayton, 3168, Victoria, Australia

[2]Water Studies, School of Chemistry, Monash University, Clayton, 3800, Victoria, Australia

[3]Department of Civil and Environmental Engineering, KAIST, Daejeon, 34141, South Korea

*Corresponding authors:
Professor Chris Greening, Department of Microbiology, Biomedicine Discovery Institute, Monash University, Clayton, Victoria, 3168, Australia. Email: chris.greening@monash.edu;
Thanh Nguyen-Dinh, Department of Microbiology, Biomedicine Discovery Institute, Monash University, Clayton, 3168, Victoria, Australia. Email: dinh.nguyen2@monash.edu.

Abstract

Nearly one-fifth of global emissions of the potent greenhouse gas nitrous oxide (N_2O) originate from the ocean, particularly from nutrient-polluted coastal regions. Permeable (sandy) sediments, which cover half of the continental shelf worldwide, are potential sources of N_2O due to increasing nutrient inputs from urbanization and agriculture. Yet, the microbial processes determining N_2O emissions in these dynamic and unique ecosystems remain understudied. Here, we combined environmental measurements, bacterial cultivation, and genomic analyses to understand the microbes and processes controlling N_2O cycling in permeable sediments from Port Phillip Bay (Australia). We established a genomic resource comprising 249 metagenome-assembled genomes and 95 new isolate genomes. Genome-based metabolic reconstructions and culture-based gas measurements revealed diverse bacteria in these sediments produce N_2O through incomplete denitrification pathways. However, these bacteria co-occurred with highly abundant clade II N_2O-reducing bacteria from the *Flavobacteriaceae* family. Kinetic profiling revealed both clade II *nosZ* flavobacterial isolates and whole sand communities exhibit a low affinity for N_2O, contrary to previous reports that clade II N_2O reducers

generally have a high substrate affinity. This indicates adaptation to the high residence times of N_2O within production and consumption zones in the sands. Collectively, these N_2O reducers remove most N_2O produced in permeable sediments, supporting lower-than-expected coastal emissions predicted by biogeochemical models. We conclude that permeable sediments host specialised microbial communities that mitigate N_2O emissions and buffer marine nitrogen cycling amid rising nutrient pollution.

Introduction

Nitrous oxide (N_2O) is a long-lived atmospheric trace gas contributing to stratospheric ozone depletion and climate change [1]. With a warming potential approximately 300 times higher than that of carbon dioxide on a 100-year time scale, N_2O is the third largest contributor (6.4%) to total greenhouse gas emissions after CO_2 and CH_4 [2,3]. Up to 57% of the total N_2O emissions come from natural sources, in which marine ecosystems contribute to nearly half of such emissions at 2-7 Tg N year^{-1} [4]. Estuarine and coastal zones function as a natural biofilter, removing excess nutrients at the interface between land and ocean [5]. However, increasing anthropogenic activities, such as nutrient loading, aquaculture and fertiliser use, are inputting nitrogen to these ecosystems, which in turn results in widespread eutrophication and exacerbates N_2O emissions [4,6–9]. N_2O emissions from coastal environments remain insufficiently understood and poorly quantified in global N_2O budgets due to complex N_2O production pathways and high spatiotemporal variability [7,10,11].

Permeable sediments (i.e. sands and gravels) dominate coastal regions, covering nearly half of the continental shelf worldwide [12]. These sediments are subject to highly turbulent hydrodynamic conditions that vary across space and time, as opposed to fine-grained impermeable (cohesive) sediments [13–15]. Advective pore-water flows drive continuous exchange of dissolved solids and gases, suspended particles and microorganisms between the sediment and overlying water column, making redox conditions in the sediments highly variable over short distances and timescales [13–15]. With microbial abundance of ~10^9 cells cm^{-3} sediments [16], sands affect N_2O emissions in coastal regions due to enhanced microbial nitrogen

cycling linked to anthropogenic nitrogen inputs. Nitrification and denitrification are the two main microbial processes that control the N_2O budget in aquatic environments [17,18]. In well-oxygenated waters, N_2O can be released by ammonia-oxidizing bacteria (AOB) and archaea (AOA) as a byproduct of ammonia oxidation to nitrite (NO_2^-) (i.e. the first step of nitrification) [9,18]. By contrast, N_2O is produced as an intermediate during denitrification of nitrate (NO_3^-) or NO_2^- under oxygen-depleted conditions [17,19]. Many denitrifiers lack the genetic capacity for N_2O reduction, resulting in N_2O released as the final product instead of inert dinitrogen gas (N_2) [20,21]. Furthermore, abiotic processes, such as (photo)-chemodenitrification, can also contribute to the production of N_2O in marine waters and sediments [22,23].

Despite several processes leading to N_2O production, the major biological sink of this gas is its reduction to dinitrogen gas (N_2) by microorganisms expressing the periplasmic, copper-containing enzyme N_2O reductase (NosZ) [24,25]. Phylogenetic analyses resolve the enzyme into clade I (NosZI), clade II (NosZII) and the recently defined clade III (NosZIII) [26–28]. NosZI is often associated with complete denitrifiers. In contrast, NosZII is found in much more diverse microbial taxa that typically lack key denitrification enzymes (i.e. NirK and NirS), suggesting N_2O serves as an electron acceptor even for non-denitrifiers [27–29]; for example, some non-denitrifying bacteria encoding the NosZII, including the acidophilic bacterium *Desulfosporosinus nitrosoreducens* [30] and methanotrophs *Methylocella tundrae* and *Methylacidiphilum caldifontis* [31], reduce N_2O to conserve energy through anaerobic respiration, while others use it to dispose excess electrons during transient anoxia (Park et al., 2017). Beyond these two clades, a recent study discovered a widespread and active clade III lactonase-type NosZ that is divergent in sequence but similar in structure to NosZI and NosZII [26]. These findings have expanded our understanding on the diversity of N_2O reducers and provide opportunities for mitigating N_2O emissions.

Given the global extent of permeable sediments, any imbalances between N_2O production and consumption can greatly impact marine N_2O budgets. While there is evidence that these sediments are a potential source of N_2O [32–36], recent hydrodynamic-biogeochemical models suggest that their contribution to coastal N_2O

emissions are relatively minor [37], highlighting uncertainties in the N_2O budget of these sediments. Furthermore, current understanding of the microbial basis of N_2O cycling within permeable sediments is largely limited to community surveys [33], with little functional and ecophysiological characterization. In this study, we addressed these knowledge gaps by investigating the functional diversity and capacity of N_2O-cycling microorganisms in sandy sediments from moderate to high nutrient-impacted beaches in Port Phillip Bay, Australia. To do so, we integrated bacterial cultivation, metagenomic analyses, and biogeochemical assays to provide a newly compiled genome collection of microorganisms inhabiting permeable sediments and assess their role in N_2O cycling. Altogether, we demonstrate that diverse N_2O producers and consumers are present and active in coastal sediments, with their tight coupling buffering the N_2O emissions from these sediments. These findings provide microbial evidence supporting hydrodynamic models [37] that coastal N_2O emissions may be overestimated and reveal new mediators of nitrogen and greenhouse gas cycling in marine ecosystems.

Results

Microbial communities in permeable sediments rapidly consume high concentrations of N_2O

To determine whether N_2O production occurs *in situ,* we measured N_2O in pore waters of subtidal sandy sediments at St. Kilda and Werribee beaches located in Port Phillip Bay, a nitrogen-limited marine embayment in Victoria, Australia. Trace amounts of N_2O (~ 0.0055 μM or 84.6% saturation) were detected in some samples; however, N_2O was generally below the limit of detection (0.004 μM dissolved gas concentration) in porewater across most sampling depths and times (**Fig. S1, Table S9**). The absence of detectable *in situ* N_2O concentrations is surprising given the denitrification activity previously reported at the same studied sites [38,39]. This may reflect three possibilities (or a combination of): (1) denitrification steps are tightly coupled, producing minimal N_2O and efficiently reducing it to N_2, (2) N_2O is only sporadically produced when NO_3^- is transported into anoxic zones or (3) non-denitrifying bacteria with clade II N_2O reductases rapidly consume N_2O produced by other community members.

We performed a series of slurry experiments to determine whether microbial communities within permeable sediments consume N_2O at a range of concentrations. Under anoxic conditions, microbial communities in the slurries rapidly consumed 0.8 μM and 108 μM N_2O with the average rates of 0.65 and 49.8 nmol h^{-1} g^{-1} wet sediment, respectively (**Fig. 1A**). Additionally, Werribee slurries showed significantly higher N_2O consumption rates (P = 0.015 - Student's t-test) than St. Kilda slurries at both concentrations, potentially reflecting long-term enrichment of denitrifying populations in these sediments at the vicinity of a wastewater treatment plant. Kinetic experiments were used to determine whether beach sand microbial communities are adapted to high or low N_2O concentrations. N_2O reduction by the sedimentary communities followed Michaelis-Menten-type kinetics (R^2 = 0.99 for St Kilda, 0.93 for Werribee) with apparent half-saturation constants [$K_{m(app)}$] of 43 and 55 μM N_2O respectively and maximum reduction rates [$V_{max\ (app)}$] of 19.6 and 46.3 nmol N_2O h^{-1} g^{-1} wet sediment (**Fig. 1B**). The [$K_{m(app)}$] values observed in this study are unusually high for marine communities, for example being orders of magnitude higher than those observed in anoxic estuarine water in Chesapeake Bay, US (0.647 μM N_2O) [25] or those in the oxic-anoxic interface from the eastern Pacific oxygen minimum zone (0.334 μM N_2O) [40]. This suggests that microbial communities within sands are exposed to much higher N_2O fluxes compared to the water column, presumably due to nutrient enrichment in these ecosystems. Furthermore, the [$V_{max(app)}$] for N_2O reduction in these sediments were one order of magnitude higher than previously reported [$V_{max(app)}$] values for denitrification in permeable sediment in Port Phillip Bay (0.5 – 5 nmol g^{-1} h^{-1}) [39], implying the capacity for N_2O consumption exceeded N_2O production in these sediments. Altogether, our results demonstrate that while permeable sediments could potentially produce elevated N_2O levels due to nutrient enrichment, rapid microbial consumption helps prevent N_2O accumulation and emissions. Thus, these sediments may function as hotspots of N_2O turnover, acting as a dynamic sink despite high N_2O exposure.

Permeable sediments host diverse N_2O producers and consumers

We used genome-resolved metagenomics to better understand the microbial and enzymatic mediators of N_2O cycling in permeable sediments. We sequenced and performed *de novo* co-assembly and binning of metagenomes from the Werribee and St. Kilda beaches, yielding 53 medium-quality and 17 high-quality metagenome-assembled genomes (MAGs). We additionally reanalysed 179 MAGs we previously obtained from St. Kilda permeable sediments [38,41] (**Table S3**). Overall, the resultant 249 MAGs span 19 phyla and 74 orders including the most abundant taxa previously reported for permeable sediment (e.g. *Woeseiaceae*, *Rhodobacteraceae* and *Flavobacteriaceae*) (**Fig. 2B, Table S3**). We then annotated the short reads, derived MAGs and unbinned contigs to determine the functional capacities and diversity of the permeable sediment microbiome.

In line with previous studies [38,41], microbial communities within permeable sediments have high capacity for denitrification. Specifically, many community members are predicted to mediate NO_3^- reduction via Nar and Nap (St. Kilda: 44%; Werribee: 58%), NO_2^- reduction via NirS and NirK (St. Kilda: 27%; Werribee: 54%) and nitric oxide (NO) reduction to N_2O via Nor (St. Kilda: 22%; Werribee: 24%) (**Fig. 2A; Table S2**). Metabolic reconstruction showed that 76 MAGs (30%) encode partial denitrification pathways, i.e. MAGs missing one or more denitrifying reductases (**Table S3**). To minimize artefacts of missing genes due to fragmented genomes, we performed more focused analyses of 64 high-quality MAGs (>90% genome completeness) to more reliably infer partial denitrification pathways. Among these, 16 MAGs were found to possess one or more denitrying reductases but lack the N_2O reductases. MAGs associated with *Arenicellaceae* (Gammaproteobacteria), *JABDKV01* (Gammaproteobacteria) and *Pyrinomonadaceae* (Acidobacteriota) families encoded Nor for N_2O production, suggesting these microorganisms are N_2O producers within the sand communities. Compared to denitrification, fewer community members mediate nitrification via Amo and Nxr (St. Kilda: 0.4%; Werribee: 8%) or dissimilatory nitrate reduction to ammonium (DNRA via Nrf – St. Kilda: 13%; Werribee: 9%) (**Fig. 2A; Table S2**).

Consistent with our activity measurements, analysis of metagenomic short reads shows that many bacteria encode genes to reduce N_2O via NosZ (St. Kilda: 23.3%; Werribee: 29.1%; **Fig. 2A**). In detail, bacteria encoding the NosZII are more abundant than the NosZI (19.6% and 20.2% versus 3.5% and 8.7% of St. Kilda and Werribee communities, respectively) while only a minor fraction of the community (St. Kilda: 0.01%; Werribee: 0.8%) encoded the NosZIII (**Fig. 2A**). Consistently, at the MAG level, only five MAGs associated with Pseudomonadota (n = 4) and Verrucomicrobiota (n = 1) encode NosZI whereas 61 MAGs spanning 8 phyla encode the NosZII (**Fig. 2B**). Of NosZII containing MAGs, 49 (80%) were Bacteroidota and 57% of these were *Flavobacteriaceae* family. Furthermore, the majority of NosZII harbouring MAGs (79%) contained only *nosZ* but not any other denitrifying genes, suggesting these microbial groups only consume, but do not produce N_2O.

To gain further insight into the phylogenetic diversity of the N_2O-reducers, we constructed a phylogenetic tree of NosZ including 647 amino sequences retrieved from 36 isolate genomes, 24 MAGs, 245 unbinned contigs, and 342 reference sequences (**Fig. 3**). Consistent with previous findings [27,29,42,43], our phylogenetic tree revealed that the NosZI is predominantly restricted to the Pseudomonadota, whereas the NosZII showed broader taxonomic distribution across several phyla (**Fig. 3**). Most NosZII sequences affiliate with Bacteroidota, specifically the family *Flavobacteriaceae* (**Fig. 3**). NosZII sequences were also affiliated with other phyla, including Gemmatimonadota, Acidobacteriota and Chloroflexota. While the NosZIII was reported to be associated with diverse taxa [26], this gene was not detected in the isolate genomes or assembled contigs in our dataset, suggesting low prevalence of clade III N_2O reducers in the studied sandy sediments.

An isolate collection of marine microbes uncovers novel mediators of N_2O cycling

To complement the metagenomic insights into the potential mediators of N_2O cycling, we conducted an isolation campaign to obtain high-quality genomes, confirm metabolic activities, and gain ecophysiological insights into key N_2O cycling

microorganisms. To the best of our knowledge, this cultivation effort generated the largest collection of permeable sediment isolates (n = 95) to date. These spanned four main phyla, including Bacillota (n = 6), Actinobacteriota (n = 4), Bacteroidota (n = 36), Alphaproteobacteria (n = 29) and Gammaproteobacteria (n = 20). These isolates represent a considerable fraction of the community's phylogenetic diversity observed from metagenome-resolved data, including dominant lineages. Based on GTDB, our isolate collection includes two novel bacterial genera and 57 novel bacterial species (**Fig. 2B, Table S4**).

Among these isolates, 12 *Alphaproteobacteria* (*Rhodobacteraceae*, n = 5) and 7 *Gammaproteobacteria* encode a complete set of denitrifying genes, including clade I *nosZ*, indicating capacity to completely reduce NO_3^- to N_2. Another 12 proteobacterial isolates encode denitrification genes except *nosZ*, suggesting they produce N_2O through partial denitrifications. The partial denitrification phenotype was experimentally validated in two isolates, an *Antarctobacter* sp. and *Sedimentitalea* sp. of the *Rhodobacteraceae* family (Alphaproteobacteria) (**Fig. 4**). The *Antarctobacter* sp. has the genomic capacity to mediate stepwise NO_3^- reduction to N_2O ($NO_3^- \rightarrow NO_2^- \rightarrow NO \rightarrow N_2O$) via Nar, NirK, and Nor, while *Sedimentitalea* sp. is predicted to only mediate NO_2^- reduction to N_2O ($NO_2^- \rightarrow NO \rightarrow N_2O$) via NirS and Nor (**Fig. 4B, C**). Consistently, the *Antarctobacter* sp. isolate completely reduced 917 ± 30 µM NO_3^- to N_2O after 24 hours of incubation with the expected 1:1 stoichiometry, after transiently producing small quantities of NO_2^-. As expected, the strain also produced N_2O when supplemented with NO_2^-; however, this was a less efficient process and only ~62% of the initial NO_2^- was reduced to N_2O after 24 hours of incubation, suggesting delayed NO reduction (**Fig. 4B**). Also consistent with the genomic predictions, the *Sedimentitalea* sp. isolate could not consume NO_3^- but did convert NO_2^- to N_2O after an initial lag (**Fig. 4C**). Given both isolates lacked the N_2O reductases, they were unable to perform the last step of denitrification and thereby emitted N_2O as their primary end product.

On the other hand, most isolates showed widespread capacity for N_2O reduction. Clade I *nosZ* genes were identified in the 12 Proteobacteria capable of complete denitrification. In contrast, clade II *nosZ* genes were identified in 20 *Flavobacteriaceae* and three *Cyclobacteriaceae* isolates (Bacteroidota). Among

these, four encoded the clade II *nosZ* without any denitrifying genes, while 16 co-encoded *nosZ* with *nor* for NO reduction to N_2O. Notably, some *Flavobacteria*ceae isolates (e.g. *Lutibacter* sp., *Algibacter* sp. and *Winogradskyella* sp.) also encoded *nrf* for DNRA whereas others (e.g. *Arenibacter algicola* or *Xanthomarina* sp.) also encoded the *nirK* genes for NO_2^- reduction. Whereas metagenomic predictions indicate that the most dominant *Flavobacteriaceae* lineages within permeable sediments are exclusive N_2O reducers, results from microbial isolates suggest that *Flavobacteriaceae* members can variably mediate NO_2^- reduction, DNRA along with N_2O reduction.

Further genomic analyses on these isolates revealed their broader metabolic breadth (**Table S4**). Most of them encode multiple terminal oxidases for aerobic respiration while some (e.g. *Lutibacter* sp. or *Oceanimonas* sp.) also encode group 3b or 3d [NiFe]-hydrogenases, which contribute to fermentative H_2 production within these sediments as previously reported [14]. This suggests that N_2O-cycling microorganisms can be extremely versatile switching between aerobic respiration, anaerobic respiration and fermentation depending on availability of electron acceptors. Additionally, many isolates encode sulfide-quinone oxidoreductase (Sqr) for sulfide oxidation, while others encoded carbon monoxide dehydrogenase for trace gas oxidation or rhodopsin for phototrophy, suggesting permeable sediment microbes can variably use organic, inorganic and solar energy sources. Altogether, these culture-based insights support our previous genome-resolved metagenomic predictions [38,41] that permeable sediment microorganisms are highly metabolically flexible, possibly as a response to frequent environmental fluctuations.

Clade II *nosZ* encoding bacteria from permeable sediments show low affinity towards N_2O

To further determine the physiological characteristics of N_2O reducers in permeable sediments, we investigated N_2O consumption by four marine bacterial isolates capable of aerobic organoheterotrophic growth. Two strains, *Olleya marilimosa* and *Winogradskyella* sp. (both *Flavobacteriaceae*), carry the clade II *nosZ* gene but lack key denitrification genes (i.e. *nirS* or *nirK*). In contrast, *Marinobacter adherens*

(Oleiphilaceae) and *Oceanimonas* sp. (*Aeromonadaceae)* carry denitrification genes and clade I *nosZ* (**Fig. 5A**). These four isolates grew aerobically in Difco 2216 Marine Broth using yeast extract and peptone as the carbon and energy sources and quickly reduced all headspace N_2O under anoxic conditions (**Fig. 5B, C, D and E**). Whole-cell kinetic measurements revealed that N_2O reduction followed Michaelis-Menten-type kinetics in all isolates (**Fig. 5B, C, D and E**). The mean apparent half-saturation constants [$K_{m(app)}$] of clade I *nosZ* strains *M. adherens* and *Oceanimonas* sp. were 94.4 µM (95% CI: 47 - 230) and 34.1 µM (95% CI: 19 - 72). In contrast, [$K_{m(app)}$] values of clade II *nosZ* flavobacterial isolates *O. marilimosa* and *Winogradskyella* sp. were considerably lower at 10.1 µM (95% CI: 3.9 – 25) and 11.3 µM (95% CI: 5.6 – 22.3), respectively.

We subsequently compared the N_2O sink strength of our permeable sediment isolates with previously characterized N_2O reducing bacteria from other ecosystems (**Fig. 6**). Clade II *nosZ* flavobacterial isolates in this study had much higher [$K_{m(app)}$] values than most clade II *nosZ* microorganisms reported to date such as *Anaeromyxobacter dehalogens* (1.34 µM) [44] or *Dechloromonas aromatica* RCM (0.324 µM) [45] (**Fig. 6A)**, indicating a relatively low affinity for N_2O. In addition to substrate affinity, we also compared their 'catalytic efficiencies' (V_{max}/K_m) to understand their ability to reduce N_2O under low N_2O concentrations (**Fig. 6B**). While the maximum reduction rates (V_{max}) of our isolates (except the clade I NosZ containing *M. adherens*) were comparable to the average of the other bacteria, their 'catalytic efficiencies' (V_{max}/K_m) was low due to their low apparent affinity towards N_2O (**Fig. 6B, Table S5**). These results suggest that, among known N_2O reducing bacteria, our isolates have relatively weak N_2O sink strength under both high and low substrate conditions regardless of their clade type.

Discussion

Through integrative approaches, we demonstrate that N_2O cycling in permeable sediment is mediated by a delicate balance between microbial production and consumption. Consistent with previous studies [33,38,41], our results show that permeable sediments host diverse microorganisms with partial denitrification

pathways (i.e. lacking one or more genes required for complete denitrification). Some of the most abundant members of the community (e.g. *Rhodobacteraceae* members) possessed either nitrite reductase and/or nitric oxide reductase, but lacked NosZ, thus producing N_2O as the terminal product of denitrification and contributing to N_2O emissions. Furthermore, we experimentally confirmed this partial genotype in two *Rhodobacteraceae* isolates (i.e. *Antarctobacter* sp. and *Sedimentitalea* sp.), which produced N_2O from either NO_3^- or NO_2^- without further reducing it to N_2, validating metagenomic and culture-based genomic predictions. At the ecosystem level, denitrification is recognized as a collective effort performed by different community members and partial denitrification can be more common across diverse terrestrial and aquatic environments [21,51,52]. Partitioning of denitrification steps among community members could alleviate competition between enzymes acting on the same substrates and enhance community flexibility and resilience under environmental disturbances [51]. Furthermore, specialising in a certain step allows partial denitrifiers to minimise resource allocation to denitrification, enabling broader metabolic flexibility to adapt to complex, dynamic and oligotrophic ecosystems [52]. Given that permeable sediments are highly dynamic with strong spatiotemporal variation in electron donor and acceptor availability, partial denitrification is more prevalent than complete denitrification in these systems. Although we did not directly measure N_2O production rates in this study, the high [$K_{m(app)}$] values for N_2O reduction of St. Kilda and Werribee sediments suggest that the N_2O reducing community in these sites is adapted to high N_2O concentrations potentially generated by these partial denitrifiers.

Despite substantial capacity for N_2O production, we provide biogeochemical, metagenomic and culture-based evidence that most N_2O is consumed by the sediment community before being emitted into the atmosphere. A diverse consortium of N_2O-reducing microorganisms carrying the clade I and II *nosZ* gene were detected, which efficiently reduce N_2O to N_2 before being released into the atmosphere. These microorganisms span several phyla including Bacteroidota, Pseudomonadota, Campylobacterota, and Gemmatimonadota, with metabolically versatile members of the *Flavobacteriaceae* (Bacteroidota) carrying clade II *nosZ* genes particularly dominant. Our results indicate that most flavobacterial isolate genomes and MAGs lack canonical genes required for dissimilatory denitrification,

suggesting that these bacteria are unlikely to produce N_2O via the conventional denitrification pathway. Instead, by expressing the clade II *nosZ* gene, they function as N_2O respirers that scavenge N_2O generated by other microorganisms. Moreover, their N_2O reducing capacity, together with the ability to use diverse energy sources, electron donors, and electron acceptors, reflects their metabolic flexibility that allows them to thrive under frequent oxic-anoxic shifts of these sediments. In this study, clade III *nosZ* was scarcely detected in the top sediment layers. Previous work has suggested that clade III *nosZ* carrying bacteria, such as members of Desulfobacterota or Nitrospinota phyla, are more likely to inhabit anoxic environments [26], whereas the highly dynamic redox conditions of permeable sediments likely limit their occurrence.

In rippled permeable sediments where solutes such as NO_3^- and N_2O are continually exchanged via advective porewaters [9,53], N_2O-reducing microorganisms might be expected to rapidly scavenge N_2O with great sink strength. This hypothesis also stemmed from our observation of few detectable *in situ* N_2O concentrations, suggesting that N_2O reducers efficiently consume N_2O as it is produced, preventing its accumulation in the environment. However, contrary to our hypothesis, our physiological work demonstrates that bacterial isolates from permeable sediments exhibited relatively weak N_2O-reducing capacity, as reflected in both average maximum reduction rates (V_{max}) and low catalytic efficiency (V_{max}/K_m) compared with other known N_2O-reducing bacteria. This unexpected finding raises questions about the mechanisms regulating N_2O cycling within these sediments. The relatively weak sink strength of these isolates may likely reflect their adaptation to the physical characteristics of these sediments. Reactive transport models have suggested that the majority of denitrification in permeable sediments is driven by NO_3^- fed from overlying water [54,55]. In these sediments, advective flow and transport dynamics can restrict interactions between oxic and anoxic zones [54]. As a result, under calm conditions without physical disturbances such as intense waves, once NO_3^- enters the reduced reaction zone and is denitrified to N_2O, long residence time would allow N_2O reducers to fully reduce N_2O to N_2 without the need to invest in high-affinity or high-rate N_2O reductases. This aligns with previous model predictions showing minimal N_2O efflux under calm wave conditions which are predominant at these studied sites, correlating with high Damköhler number, a dimensionless ratio of

reaction to transport rates [37]. Under more hydrodynamically active conditions, more oxygen is introduced into the sediment, limiting the opportunities for denitrification and N_2O production to take place. It is only under specific intermediate conditions of sediment flushing that significant amounts of N_2O escapes the sediment, making it a rare occurrence (<3% of the time) [37].

Altogether, our findings suggest a potential cross-feeding interaction between N_2O producers and non-denitrifying N_2O reducers, which efficiently buffers the emissions of this potent greenhouse gas in eutrophic permeable sediments. The efficiency of N_2O removal by clade II N_2O-reducing bacteria may be attributed to the unique physical characteristics of these sediments rather than their biokinetic parameters. This suggests that physical characteristics of these sediments not only influence dynamics of greenhouse gases, but also drive the adaptation and ecophysiological strategies of resident microbial communities. Future work should investigate how these microorganisms respond and mediate N_2O emissions under variable hydrodynamic regimes.

Materials and Methods

Sampling and *in situ* N_2O level measurements

Different sampling campaigns were conducted at St. Kilda Beach (37.863159°S, 144.971026°E) and Werribee Beach (37.58132°S, 144.42112°E) between 2022 and 2024 for different purposes: i) bacterial isolation (02/06/2022, 03/08/2022, 19/10/2022 and 11/01/2023), ii) slurry incubations (10/05/2024 for St. Kilda samples; 23/09/2024 and 20/08/2025 for Werribee samples) and iii) *in situ* N_2O concentrations (24/05/2024, 05/11/2024 for Werribee and 15/05/2024, 01/10/2024 and 18/11/2024 for St. Kilda). Subtidal surface sediment (0-5 cm deep) was collected in sterile 50 mL Falcon tubes and were immediately transported to the laboratory and stored at 4°C overnight before experiments. The sediments for metagenomic sequencing were also sub-sampled, flash-frozen in liquid nitrogen and stored at -20°C until further analysis. Seawater samples were collected for slurry incubations and were filtered (0.22 µm) to remove most pelagic species. *In situ* N_2O levels were measured from

pore-water samples collected with a piezometer connected with a rubber tube and over-filled in 12 mL exetainers. Three replicates were collected, each spaced 2 m apart. Samples were preserved by adding 50 µL saturated $HgCl_2$ and stored at room temperature. For dissolved N_2O concentration measurement, a 4 mL helium headspace was introduced into each 12.5 mL Exetainer vial, shaken and equilibrated at room temperature before being analysed by gas chromatography described below.

Slurry incubations

Sediment experiments were conducted in order to determine N_2O consumption capability of the sediment community. Slurries were prepared with 5 g of wet sediment and 50 mL filtered seawater in 120 mL serum vials before sealing with a butyl rubber stopper (Sigma-Aldrich) and Wheaton closed-top seals (Sigma-Aldrich). Serum vials were purged with helium (He) gas for 10 minutes with vigorous shaking every five minutes to exclude O_2 and create anoxic conditions. The headspace of vials was amended with N_2O (Air Liquide Australia Limited) to give initial mixing ratios of approximately 10 (0.8 μM) or 1,000 ppmv (108 μM). Before measurement, 2 mL He was injected into the headspace, then 2 mL of sample was taken from the headspace and injected into a He pre-purged 3 mL exetainer. Samples were analysed using a VICI Trace Gas Analyser with a limit of detection of 0.05 ppmv.

Metagenomic sequencing and assembly

Environmental DNA was extracted from six sediment samples collected at St.Kilda and Werribee Beach using the PowerSoil® DNA kit (QIAGEN) following the manufacturer's instructions. Extractions included a sample-free negative control. Samples were sequenced on an Illumina NovaSeqX Plus (2 × 150 bp) at Monash Genomics & Bioinformatics Platform (Monash University). Sequencing yielded an average of 44,021,402 read pairs per sample, with 1,052 read pairs sequenced in the negative control. The metagenomes were processed using the Metaphor workflow [56]. Specifically, the metagenomes were quality filtered with fastp [57] and co-assembled using MEGAHIT v1.2.9 [58] with default settings. Contigs shorter than 1,000 bp were discarded. The assembled contigs were binned with Vamb v4.1.3 [59],

MetaBAT v2.12.1 [60] and CONCOCT v1.1.0 [61]. The three bin sets were subsequently refined using DAS Tool v1.1.6 [62], combined with MAGs previously obtained from St. Kilda permeable sediments [38,41] and dereplicated with dRep v3.4.2 [63] using the parameters -comp 50 -con 10. The completeness, contamination and heterogeneity of the bins were assessed using CheckM2 [64]. Quality thresholds for bins were set as per MIMAG standards [65], retaining only medium (completeness >50%, contamination <10%) and high (completeness >90%, contamination <5%) quality bins for further processing, which were termed metagenome-assembled genomes (MAGs). MAG taxonomy was determined using the Genome Taxonomy Database Release R226 [66] via GTDB-Tk v2.3.2 [67]. CoverM [68] with the option 'genome' was used to calculate the relative abundance of each MAG in each sample.

Bacterial isolation and whole genome analysis

Sediment samples for bacterial isolation were collected at St. Kilda Beach in three sampling campaigns (02/06/2022, 03/08/2022 and 11/01/2023) and at Werribee Beach (19/10/2022). Approximately 1 g wet weight of the surface sediment (0-5 cm deep) was dispersed in 9 mL of sterilised 1× phosphate-buffered saline (PBS), vortexed vigorously for three minutes and sonicated for another three minutes. The resulting slurry was serially diluted with 1× PBS and stored in cryovials at -80 ^{o}C with 25% glycerol for further isolation if needed. Aliquots of 100 µL undiluted and serially diluted slurry were spread on Marine Agar 2216 (Difco), modified Marine Agar 2216E, and Marine R2A Agar plates (ingredients in **Table S1**) and incubated aerobically at 30 ^{o}C for at least one week until most morphologically different colonies appeared on the plates. A series of enrichments were also performed using 1 mM $NaNO_3$ or $NaNO_2$ as electron acceptors and either 1 mM sodium acetate, 1 mM glucose, 0.002 g/L starch or 0.5 g/L yeast extract as electron donors. Approximately 5 g of sediments were suspended in 50 mL of a bicarbonate-buffered minimal saltwater medium (MSW) (**Table S1**) in 120-mL serum bottles and purged with N_2 for three minutes to create anoxic conditions. Enrichments were transferred to fresh medium when NO_3^-/NO_2^- was all consumed, using 10% inoculum (v/v). After the third transfer, the slurries were serially diluted, isolated by streaking on Marine Agar 2216 or MSW agar and incubated at the same conditions as mentioned above. Bacterial stocks were preserved at -80 ^{o}C in 25% glycerol for long-term storage. For

isolate identification, DNA was extracted by heating 30 µL of colony suspension at 95°C for 15 minutes and immediately frozen at -20°C and the 16S rRNA gene was amplified using the universal eubacterial primers 27F (5'-AGA GTT TGA TCC TGG CTC AG-3') and 806rB (5'-GGA CTA CNV GGG TWT CTA AT-3') or 1492R (5'-GGT ACC TTG TTA CGA CTT-3'). Purified PCR products were Sanger sequenced (Monash Genomics & Bioinformatics Platform, Victoria, Australia) and the obtained sequences were compared with those available in the GenBank database using BLAST on NCBI (National Center for Biotechnology Information) website.

A total of 95 bacterial isolates from permeable sediments collected in St. Kilda and Werribee beaches were selected for whole genome sequencing. The genomic DNA of isolates was extracted using the Genomic DNA Kit (Meridian Bioscience) following the manufacturer's instructions. Samples were sequenced on Illumina NovaSeq 6000 platform at GENEWIZ (AZENTA Life Sciences). Raw sequences were quality filtered with the BBTools suite v.38.81 (https://sourceforge.net/projects/bbmap/), using BBDuk to remove the 151st base, trim adapters, filter PhiX reads, trim the 3' end at a quality threshold of 15 and discard reads below 50 bp in length. Processed short reads were assembled using Unicycler v.0.4.7 [69]. The assembled genome quality was assessed with CheckM2 [64] and taxonomic classification of each isolate was performed using GTDB-tk v2.1.1 [67].

Metabolic annotation

Open reading frames (ORFs) were predicted using Prodigal v2.6.3 [70] for isolate whole genome and MAGs, then annotated using DIAMOND v2.0.15 [71] for alignment against a custom set of 51 metabolic marker protein databases (https://doi.org/10.26180/c.5230745) covering the major pathways for aerobic and anaerobic respiration, energy conservation from organic and inorganic compounds, carbon fixation, nitrogen fixation and phototrophy. Gene hits were filtered by a minimum percentage identity score by protein: 80% (PsaA), 75% (HbsT), 70% (PsbA, IsoA, AtpA, YgfK and ARO), 60% (CoxL, MmoX, AmoA, NxrA, RbcL, NuoF, [FeFe]-hydrogenases and NiFe Group 4 hydrogenases) or 50% (all other genes). To determine gene abundance in the community, read counts of each gene were normalized to reads per kilobase million (RPKM) and then divided by the mean

abundance of 14 universal single-copy ribosomal marker genes (in RPKM, obtained from the SingleM v0.13.2 package) [72].

Phylogenetic analysis

To understand the distribution and diversity of microorganisms in marine permeable sediments involved in the nitrogen cycling and N_2O emission, a phylogenomic tree was constructed from 95 bacterial isolate whole genomes and 97 MAGs. Genomes were aligned based on the AR53/BAC120 marker set of GTDB-Tk (v2.4.0) using the "align" option and the tree was generated by maximum likelihood estimation with the ultrafast bootstrap value of 1,000 and model Q.pfam+I+G4 using IQ-TREE [73]. In addition, we also analysed the diversity of clade I and clade II *nosZ* genes present in permeable sediments. To do so, we retrieved the NosZ amino acid sequences derived from unbinned and binned contigs and isolate genomes. Any sequences shorter than 300 amino acids were excluded. We also included the NosZ amino acid sequences from the Greening Lab database (https://doi.org/10.26180/c.5230745) and clade III NosZ sequences from [26] as reference. Sequences were aligned using MAFFT v7.526 [74] and trimmed with TrimAL 1.2rev59 [75] with default settings. Maximum-likelihood trees were constructed with the ultrafast bootstrap value of 1,000 and model Q.pfam+I+G4 using IQ-TREE [73]. The tree was visualised and midpoint-rooted using the Interactive Tree of Life (iTOL) [76].

Isolate physiological characterisation

The partial denitrification phenotype was tested in two bacterial isolates (i.e. *Antarctobacter* sp. and *Sedimentitalea* sp.). The N_2O-reducing phenotype was tested in two clade II *nosZ* organisms (i.e. *Olleya marilimosa* and *Winogradskyella* sp.) and two clade I *nosZ* organisms (i.e., *Marinobacter adherens* and *Oceanimonas* sp.). All cultures were grown overnight in Difco 2216 Marine Broth medium under oxic conditions. Overnight cultures were transferred to 50 mL of fresh media so that the starting optical density (OD_{600}) reached 0.03. Oxic treatment remained as unamended air while anoxic treatments were purged with He to exclude O_2 as described above. For partial denitrification phenotype analysis, cultures were amended with either 1mM $NaNO_3$ or 0.1 mM $NaNO_2$ and the concentrations of NO_x

(NO_3^- + NO_2^-) and NO_2^- were determined spectrophotometrically on a Lachat Quickchem 8000 following the procedures in Standard Methods for Water and Wastewater [77]. Headspace gas (2 mL) was sampled into He purged 12-mL exetainers to monitor N_2O production. For N_2O reduction phenotype analysis, the headspace of anoxic vials were amended with N_2O as the main electron acceptor to give initial mixing ratios of approximately 100 and 1,000 ppmv. Vials were placed on an orbital shaker (150 rpm) at 30°C for 24 hours. To monitor N_2O concentration changes, 2 mL of headspace gas was sampled into He purged 3-mL exetainers.

Kinetic analysis

Rates of N_2O consumption by *O. marilimosa, Winogradskyella* sp., *M. adherens* and *Oceanimonas* sp. and by whole sediment communities from the two studied sites were measured. For axenic cultures, overnight-grown cells under oxic conditions (OD_{600} of 3.0 to 4.0) were inoculated into 50 mL fresh Difco Marine Broth medium in 120-mL serum vials to reach an initial OD_{6oo} of 0.03 then vials were sealed with butyl rubber stoppers. Similarly, slurry was prepared with 5 g of wet sediment and 50 mL filtered seawater in 120-mL serum vials and sealed with butyl rubber stoppers. Vials were purged with He gas to exclude O_2 as described above. Triplicate cultures or slurries were incubated with different N_2O concentrations in the headspace ranging from 5 to 1,000 ppmv. Headspace N_2O concentrations were quantified by gas chromatography at different time intervals. The final N_2O concentration in the liquid phase was corrected and calculated as previously described [78]. Reaction rates of N_2O consumption were determined from the slopes of linear regression lines fitted to N_2O concentration measurements over time. Michaelis-Menten curves and parameters were estimated using the non-linear fit (Michaelis-Menten, least squares regression) function in GraphPad Prism v10.3.1.

Data availability

All sequences generated from this work were deposited to the NCBI Sequence Read Archive under the BioProject accession numbers PRJNA1347951 for metagenomes and metagenome-assembled genomes and PRJNA1348900 for isolate whole genomes. Bacterial and archaeal MAGs generated from the same sites in previous

studies [38,41] were downloaded from NCBI Sequence Read Archive with BioProject accession number PRJNA623061 and PRJNA609151.

Conflict of interest

The authors declare no conflict of interest.

Acknowledgement

This work was supported by an ARC Discovery Project (DP210101595; awarded to P.M.L.C, C.G. and W.W.W), an ARC Future Fellowship (FT240100502; awarded to C.G), ARC Discovery Early Career Awards (DE250101210 to P.M.L., DE230100542 to R.L.), Monash International Tuition Scholarships and Monash Graduate Scholarship (awarded to T.N.D).

Author contributions

C.G, P.L.M.C and W.W.W conceived and supervised the study. Experimental planning and design were conducted by T.N.D, C.G., W.W.W. and P.L.M.C. T.N.D and L.J were responsible for bacterial isolation and culturing. T.N.D, H.P., and W.W.W. were responsible for environmental microcosms and monitoring. T.N.D. and T.F.H were responsible for physiological and kinetic characterization of isolates. Chemical analyses were performed by V.E. Metagenomic and whole genome analyses were performed by T.N.D, F.R., R.L and P.M.L. Resources, supervision and funding were contributed by C.G., P.L.M.C and W.W.W. The manuscript was written by T.N.D and F.R. with contributions from all authors.

Supplementary materials

Figure S1 | *In situ* N_2O concentrations in permeable sediments

Table S1 | Composition of different media used for isolation of bacteria from permeable sediments in St. Kilda Beach and Werribee.

Table S2 (xlsx). Sequencing statistics and abundance of metabolic marker genes in the short read metagenomic data. This includes the calculated average copies per organism for each marker gene, average copies per organism for nitrogen metabolising genes and a list of short read hits and their corresponding match in the database.

Table S3 (xlsx). Summary and annotation of dereplicated metagenome-assembled-genomes (MAGs) obtained from this study and previous [38,41] studies. This includes taxonomic information for each MAG, relative abundance of each MAG per sample calculated by CoverM, a summary of metabolic marker genes identified in each MAG, a list of clade II *nosZ* containing MAGs, a list of high-quality MAGs and a full list of metabolic marker genes identified in the MAGs with alignment information and protein sequences.

Table S4 (xlsx). Summary of bacterial isolates. This includes taxonomic information for each isolate and a summary of metabolic marker genes identified in each isolate genome.

Table S5. Comparison of biokinetic parameters for marine permeable sediment isolates and other N_2O-reducing bacteria.

Table S6 (xlsx). Sequences of metabolic genes in unbinned contigs derived from homology-based searches.

Table S7 (xlsx). Measurements of N_2O concentrations and kinetic analyses. This includes measurement of N_2O concentrations in slurries and four bacterial isolates.

Table S8 (xlsx). Measurements of NO_x and N_2O in two *Rhodobacteraceae* isolates (i.e. *Antarctobacter* sp. and *Sedimentitalea* sp.) with partial denitrification pathways.

Table S9 (xlsx). *In situ* N_2O concentrations in porewaters of St. Kilda and Werribee permeable sediments.

References

1. Ravishankara AR, Daniel JS, Portmann RW. Nitrous Oxide (N_2O): The Dominant Ozone-Depleting Substance Emitted in the 21st Century. *Science* 2009;**326**:123–5.

2. Intergovernmental Panel On Climate Change. *Climate Change 2021 – The Physical Science Basis: Working Group I Contribution to the Sixth Assessment Report of the Intergovernmental Panel on Climate Change*. 1st ed. Cambridge University Press, 2023.

3. Zhu G, Shi H, Zhong L *et al.* Nitrous oxide sources, mechanisms and mitigation. *Nat Rev Earth Environ* 2025, DOI: 10.1038/s43017-025-00707-5.

4. Tian H, Xu R, Canadell JG *et al.* A comprehensive quantification of global nitrous oxide sources and sinks. *Nature* 2020;**586**:248–56.

5. Tang W, Da F, Tracey JC *et al.* Nutrient management offsets the effect of deoxygenation and warming on nitrous oxide emissions in a large US estuary. *Sci Adv* 2024;**10**:eadq5014.

6. Beusen AHW, Doelman JC, Van Beek LPH *et al.* Exploring river nitrogen and phosphorus loading and export to global coastal waters in the Shared Socio-economic pathways. *Glob Environ Change* 2022;**72**:102426.

7. Chen C, Yin T, Yin G *et al.* Mapping N2O production pathways in estuarine and coastal sediments through coupled 15N tracing and N2O isotopocules analysis. *J Hydrol* 2024;**645**:132170.

8. Doney SC. The Growing Human Footprint on Coastal and Open-Ocean Biogeochemistry. *Science* 2010;**328**:1512–6.

9. Santos IR, Eyre BD, Huettel M. The driving forces of porewater and groundwater flow in permeable coastal sediments: A review. *Estuar Coast Shelf Sci* 2012;**98**:1–15.

10. Gu X, Wang L, Casciotti KL *et al.* Mixed Archaeal Production and Nitrifier Denitrification Dominate N_2O Production in the East China Sea: Insights From Isotopocule and Hydroxylamine Analyses. *J Geophys Res Oceans* 2023;**128**, DOI: 10.1029/2022jc019355.

11. Wan XS, Sheng H-X, Liu L *et al.* Particle-associated denitrification is the primary source of N2O in oxic coastal waters. *Nat Commun* 2023;**14**, DOI: 10.1038/s41467-023-43997-3.

12. Hall SJ. The continental shelf benthic ecosystem: current status, agents for change and future prospects. *Environ Conserv* 2002;**29**:350–74.

13. Huettel M, Berg P, Kostka JE. Benthic Exchange and Biogeochemical Cycling in Permeable Sediments. *Annu Rev Mar Sci* 2014;**6**:23–51.

14. Kessler AJ, Chen Y-J, Waite DW *et al.* Bacterial fermentation and respiration processes are uncoupled in anoxic permeable sediments. *Nat Microbiol* 2019;**4**:1014–23.

15. Precht E, Franke U, Polerecky L *et al.* Oxygen dynamics in permeable sediments with wave-driven pore water exchange. *Limnol Oceanogr* 2004;**49**:693–705.

16. Musat N, Werner U, Knittel K *et al.* Microbial community structure of sandy intertidal sediments in the North Sea, Sylt-Rømø Basin, Wadden Sea. *Syst Appl Microbiol* 2006;**29**:333–48.

17. Devol AH. Denitrification, Anammox, and N_2 Production in Marine Sediments. *Annu Rev Mar Sci* 2015;**7**:403–23.

18. Ward BB. Nitrification in Marine Systems. *Nitrogen in the Marine Environment*. Elsevier, 2008, 199–261.

19. Ward BB. How Nitrogen Is Lost. *Science* 2013;**341**:352–3.

20. Philippot L, Andert J, Jones CM *et al.* Importance of denitrifiers lacking the genes encoding the nitrous oxide reductase for N2O emissions from soil: ROLE OF DENITRIFIER DIVERSITY FOR N2O FLUXES. *Glob Change Biol* 2011;**17**:1497–504.

21. Pold G, Saghaï A, Jones CM *et al.* Denitrification is a community trait with partial pathways dominating across microbial genomes and biomes. *Nat Commun* 2025;**16**:9495.

22. Leon-Palmero E, Morales-Baquero R, Thamdrup B *et al.* Sunlight drives the abiotic formation of nitrous oxide in fresh and marine waters. *Science* 2025;**387**:1198–203.

23. Wankel SD, Ziebis W, Buchwald C *et al.* Evidence for fungal and chemodenitrification based N2O flux from nitrogen impacted coastal sediments. *Nat Commun* 2017;**8**, DOI: 10.1038/ncomms15595.

24. Müller C, Zhang L, Zipfel S *et al.* Molecular interplay of an assembly machinery for nitrous oxide reductase. *Nature* 2022;**608**:626–31.

25. Tang W, Jayakumar A, Sun X *et al.* Nitrous Oxide Consumption in Oxygenated and Anoxic Estuarine Waters. *Geophys Res Lett* 2022;**49**:e2022GL100657.

26. He G, Wang W, Chen G *et al.* A novel bacterial protein family that catalyses nitrous oxide reduction. *Nature* 2025, DOI: 10.1038/s41586-025-09401-4.

27. Jones CM, Graf DR, Bru D *et al.* The unaccounted yet abundant nitrous oxide-reducing microbial community: a potential nitrous oxide sink. *ISME J* 2013;**7**:417–26.

28. Sanford RA, Wagner DD, Wu Q *et al.* Unexpected nondenitrifier nitrous oxide reductase gene diversity and abundance in soils. *Proc Natl Acad Sci* 2012;**109**:19709–14.

29. Hallin S, Philippot L, Löffler FE *et al.* Genomics and Ecology of Novel N2O-Reducing Microorganisms. *Trends Microbiol* 2018;**26**:43–55.

30. He G, Chen G, Xie Y *et al.* Sustained bacterial N2O reduction at acidic pH. *Nat Commun* 2024;**15**:4092.

31. Awala SI, Gwak J-H, Kim Y *et al.* Nitrous oxide respiration in acidophilic methanotrophs. *Nat Commun* 2024;**15**:4226.

32. Jameson BD, Berg P, Grundle DS *et al.* Continental margin sediments underlying the NE Pacific oxygen minimum zone are a source of nitrous oxide to the water column. *Limnol Oceanogr Lett* 2021;**6**:68–76.

33. Marchant HK, Tegetmeyer HE, Ahmerkamp S *et al.* Metabolic specialization of denitrifiers in permeable sediments controls N_2O emissions. *Environ Microbiol* 2018;**20**:4486–502.

34. Marchant HK, Holtappels M, Lavik G *et al.* Coupled nitrification-denitrification leads to extensive N loss in subtidal permeable sediments: Coupled nitrification-denitrification in sands. *Limnol Oceanogr* 2016;**61**:1033–48.

35. Schutte CA, Joye SB, Wilson AM *et al.* Intense nitrogen cycling in permeable intertidal sediment revealed by a nitrous oxide hot spot. *Glob Biogeochem Cycles* 2015;**29**:1584–98.

36. Wong WW, Greening C, Shelley G *et al.* Effects of drift algae accumulation and nitrate loading on nitrogen cycling in a eutrophic coastal sediment. *Sci Total Environ* 2021;**790**:147749.

37. Fowdar H, Grant SB, Wong WW *et al.* Hydrodynamics Control Nitrous Oxide Production in Eutrophic Coastal Permeable Sediments. *J Geophys Res Biogeosciences* 2024;**129**:e2023JG007715.

38. Chen Y-J, Leung PM, Cook PLM *et al.* Hydrodynamic disturbance controls microbial community assembly and biogeochemical processes in coastal sediments. *ISME J* 2022;**16**:750–63.

39. Evrard V, Glud RN, Cook PLM. The kinetics of denitrification in permeable sediments. *Biogeochemistry* 2013;**113**:563–72.

40. Sun X, Jayakumar A, Tracey JC *et al.* Microbial N2O consumption in and above marine N2O production hotspots. *ISME J* 2021;**15**:1434–44.

41. Chen Y-J, Leung PM, Wood JL *et al.* Metabolic flexibility allows bacterial habitat generalists to become dominant in a frequently disturbed ecosystem. *ISME J* 2021;**15**:2986–3004.

42. Intrator N, Jayakumar A, Ward BB. Aquatic nitrous oxide reductase gene (nosZ) phylogeny and environmental distribution. *Front Microbiol* 2024;**15**:1407573.

43. Jiang Q, Cao L, Han Y *et al.* Cold seeps are potential hotspots of deep-sea nitrogen loss driven by microorganisms across 21 phyla. *Nat Commun* 2025;**16**:1646.

44. Suenaga T, Riya S, Hosomi M *et al.* Biokinetic Characterization and Activities of N2O-Reducing Bacteria in Response to Various Oxygen Levels. *Front Microbiol* 2018;**9**:697.

45. Yoon S, Nissen S, Park D *et al.* Nitrous Oxide Reduction Kinetics Distinguish Bacteria Harboring Clade I NosZ from Those Harboring Clade II NosZ. Kostka JE (ed.). *Appl Environ Microbiol* 2016;**82**:3793–800.

46. Hiis EG, Vick SHW, Molstad L *et al.* Unlocking bacterial potential to reduce farmland N2O emissions. *Nature* 2024;**630**:421–8.

47. Suenaga T, Hori T, Riya S *et al.* Enrichment, Isolation, and Characterization of High-Affinity N_2 O-Reducing Bacteria in a Gas-Permeable Membrane Reactor. *Environ Sci Technol* 2019;**53**:12101–12.

48. Tang W, Jayakumar A, Sun X *et al.* Nitrous Oxide Consumption in Oxygenated and Anoxic Estuarine Waters. *Geophys Res Lett* 2022;**49**:e2022GL100657.

49. Kleiner M, Thorson E, Sharp CE *et al.* Assessing species biomass contributions in microbial communities via metaproteomics. *Nat Commun* 2017;**8**:1558.

50. Milo R, Jorgensen P, Moran U *et al.* BioNumbers—the database of key numbers in molecular and cell biology. *Nucleic Acids Res* 2010;**38**:D750–3.

51. Pessi IS, Viitamäki S, Virkkala A-M *et al.* In-depth characterization of denitrifier communities across different soil ecosystems in the tundra. *Environ Microbiome* 2022;**17**, DOI: 10.1186/s40793-022-00424-2.

52. Roothans N, Van Loosdrecht MCM, Laureni M. Metabolic labour division trade-offs in denitrifying microbiomes. *ISME J* 2025;**19**:wraf020.

53. Huettel M, Ziebis W, Forster S. Flow-induced uptake of particulate matter in permeable sediments. *Limnol Oceanogr* 1996;**41**:309–22.

54. Kessler AJ, Glud RN, Cardenas MB *et al.* Transport Zonation Limits Coupled Nitrification-Denitrification in Permeable Sediments. *Environ Sci Technol* 2013;**47**:13404–11.

55. Kessler AJ, Glud RN, Cardenas MB *et al.* Quantifying denitrification in rippled permeable sands through combined flume experiments and modeling. *Limnol Oceanogr* 2012;**57**:1217–32.

56. Salazar VW, Shaban B, Quiroga MDM *et al.* Metaphor—A workflow for streamlined assembly and binning of metagenomes. *GigaScience* 2022;**12**:giad055.

57. Chen S. Ultrafast one-pass FASTQ data preprocessing, quality control, and deduplication using fastp. *iMeta* 2023;**2**:e107.

58. Li D, Liu C-M, Luo R *et al.* MEGAHIT: an ultra-fast single-node solution for large and complex metagenomics assembly via succinct *de Bruijn* graph. *Bioinformatics* 2015;**31**:1674–6.

59. Nissen JN, Johansen J, Allesøe RL *et al.* Improved metagenome binning and assembly using deep variational autoencoders. *Nat Biotechnol* 2021;**39**:555–60.

60. Kang DD, Li F, Kirton E *et al.* MetaBAT 2: an adaptive binning algorithm for robust and efficient genome reconstruction from metagenome assemblies. *PeerJ* 2019;**7**:e7359.

61. Alneberg J, Bjarnason BS, De Bruijn I *et al.* Binning metagenomic contigs by coverage and composition. *Nat Methods* 2014;**11**:1144–6.

62. Sieber CMK, Probst AJ, Sharrar A *et al.* Recovery of genomes from metagenomes via a dereplication, aggregation and scoring strategy. *Nat Microbiol* 2018;**3**:836–43.

63. Olm MR, Brown CT, Brooks B *et al.* dRep: a tool for fast and accurate genomic comparisons that enables improved genome recovery from metagenomes through de-replication. *ISME J* 2017;**11**:2864–8.

64. Chklovski A, Parks DH, Woodcroft BJ *et al.* CheckM2: a rapid, scalable and accurate tool for assessing microbial genome quality using machine learning. *Nat Methods* 2023;**20**:1203–12.

65. The Genome Standards Consortium, Bowers RM, Kyrpides NC *et al.* Minimum information about a single amplified genome (MISAG) and a metagenome-assembled genome (MIMAG) of bacteria and archaea. *Nat Biotechnol* 2017;**35**:725–31.

66. Parks DH, Rinke C, Chuvochina M *et al.* Author Correction: Recovery of nearly 8,000 metagenome-assembled genomes substantially expands the tree of life. *Nat Microbiol* 2017;**3**:253–253.

67. Chaumeil P-A, Mussig AJ, Hugenholtz P *et al.* GTDB-Tk v2: memory friendly classification with the genome taxonomy database. Borgwardt K (ed.). *Bioinformatics* 2022;**38**:5315–6.

68. Aroney STN, Newell RJP, Nissen JN *et al.* CoverM: read alignment statistics for metagenomics. Alkan C (ed.). *Bioinformatics* 2025;**41**:btaf147.

69. Wick RR, Judd LM, Gorrie CL *et al.* Unicycler: Resolving bacterial genome assemblies from short and long sequencing reads. Phillippy AM (ed.). *PLOS Comput Biol* 2017;**13**:e1005595.

70. Hyatt D, Chen G-L, LoCascio PF *et al.* Prodigal: prokaryotic gene recognition and translation initiation site identification. *BMC Bioinformatics* 2010;**11**:119.

71. Buchfink B, Xie C, Huson DH. Fast and sensitive protein alignment using DIAMOND. *Nat Methods* 2015;**12**:59–60.

72. Woodcroft BJ, Aroney STN, Zhao R *et al.* SingleM and Sandpiper: Robust microbial taxonomic profiles from metagenomic data. 2024, DOI: 10.1101/2024.01.30.578060.

73. Minh BQ, Schmidt HA, Chernomor O *et al.* IQ-TREE 2: New Models and Efficient Methods for Phylogenetic Inference in the Genomic Era. Teeling E (ed.). *Mol Biol Evol* 2020;**37**:1530–4.

74. Katoh K. MAFFT: a novel method for rapid multiple sequence alignment based on fast Fourier transform. *Nucleic Acids Res* 2002;**30**:3059–66.

75. Capella-Gutiérrez S, Silla-Martínez JM, Gabaldón T. trimAl: a tool for automated alignment trimming in large-scale phylogenetic analyses. *Bioinformatics* 2009;**25**:1972–3.

76. Letunic I, Bork P. Interactive Tree Of Life (iTOL) v5: an online tool for phylogenetic tree display and annotation. *Nucleic Acids Res* 2021;**49**:W293–6.

77. APHA. Standard methods for the Examination of Water and WasteWater. 2005.

78. Weiss RF, Price BA. Nitrous oxide solubility in water and seawater. *Mar Chem* 1980;**8**:347–59.

Figure captions

Figure 1. N_2O consumption by permeable sediments. (**A**) Anoxic slurry incubation of surface sediments (0-5 cm) from St. Kilda (13/05/2024) and Werribee (23/09/2024) with different N_2O concentrations. (**B**) Kinetics of N_2O reduction by surface sediments in St. Kilda (13/05/2024 samples) and Werribee (20/08/2025 samples). The curves were fitted and kinetic parameters were approximated based on a Michaelis-Menten non-linear regression model.

Figure 2. Nitrogen-cycling metabolic capacity of microbial communities in permeable sediments. (**A**) Relative abundance of nitrogen metabolizing genes in St. Kilda and Werribee beaches based on gene-centric metagenomic analysis (**B**) Maximum-likelihood phylogenomic tree showing nitrogen-cycling metabolic gene inventories of 95 bacterial isolates and 245 bacterial MAGs generated from this study and acquired from (Chen et al., 2022, 2021). The tree was built with 1,000 ultrafast bootstrap replicates using the LG+F+I+G4 model via IQ-TREE. Tree branches were colour-indexed to show phylum-level taxonomy of bacterial isolates and MAGs. Key metabolic genes for denitrification were highlighted using coloured rings. Specific isolates were selected for further analysis, including culture-based activity and kinetic measurements (asterisks).

Figure 3. Diversity of NosZ in permeable sediments. The maximum-likelihood phylogenetic tree of NosZ amino acid sequences was generated using Q.pfam+I+G4 substitution model (via IQ-TREE) and was midpoint rooted. The NosZ amino acid sequences derived from MAGs (n = 24) and isolate genomes (n = 36) are shown in **bold,** whereas sequences from unbinned contigs (n = 245) are marked with an asterisk (*). Additionally, 342 reference NosZ sequences were included. Taxonomic assignments are indicated by branch colours on the tree.

Figure 4. Partial denitrification genotype and phenotype of selected bacterial isolates. (A) Presence and absence of denitrifying genes in two isolates. (**B**) Partial denitrification phenotypes in *Antarctobacter* sp. (**C**) Partial denitrification phenotypes in *Sedimentitalea* sp. Both isolates were grown on Difco 2216 Marine Broth with either 1 mM $NaNO_3$ for NO_3^- treatment or 0.1 mM $NaNO_2$ for NO_2^- treatment under

anoxic conditions. Data are presented as mean ± SD, n = 3 biologically independent samples, with media-only vials (n = 2) as negative controls.

Figure 5. N_2O reduction genotype and phenotype of clade I and II N_2O reducing isolates. (A) The presence and absence of *nosZ* genes and other denitrifying genes in selected isolates based on whole genome sequencing and metabolic annotation. (**B-D**) Aerobic growth and N_2O reducing activity of *O. marilimosa* and *Winogradskyella* sp. (clade II *nosZ* isolates) and *M. adherens* and *Oceanimonas* sp. (clade I *nosZ* isolates) respectively. Isolates were grown on Difco 2216 Marine Broth aerobically or anaerobically with N_2O as the sole terminal electron acceptor. Growth was determined by optical density measurements at 600 nm, followed by measurements of N_2O concentration in the headspaces of the culture vials. Kinetics of N_2O reduction of four isolates were calculated based on a Michaelis-Menten non-linear regression model. All experiments were performed in triplicate. Data are presented as mean ± standard deviation (SD).

Figure 6. Comparison of N_2O reduction biokinetics between different N_2O reducing microorganisms. (A) Affinities for N_2O reported for N_2O-reducing isolates and whole communities from this and previous studies [40,44–48] (**B**) N_2O sink strength of various microorganisms from different ecosystems, determined by plotting the 'catalytic efficiency' (V_{max}/K_m) against the maximum reduction rates (V_{max}). To enable consistent comparison, we converted all V_{max} values to mmol N_2O g^{-1} cell dry weight h^{-1}, assuming the total protein amounts account for 55% of the total dry biomass [49,50]. We also converted all values to V_{max} at 20°C assuming the rates increase exponentially with temperature by the factor of 2.5 per 10°C increase in temperature (Q_{10} = 2.5), as previously described [46].

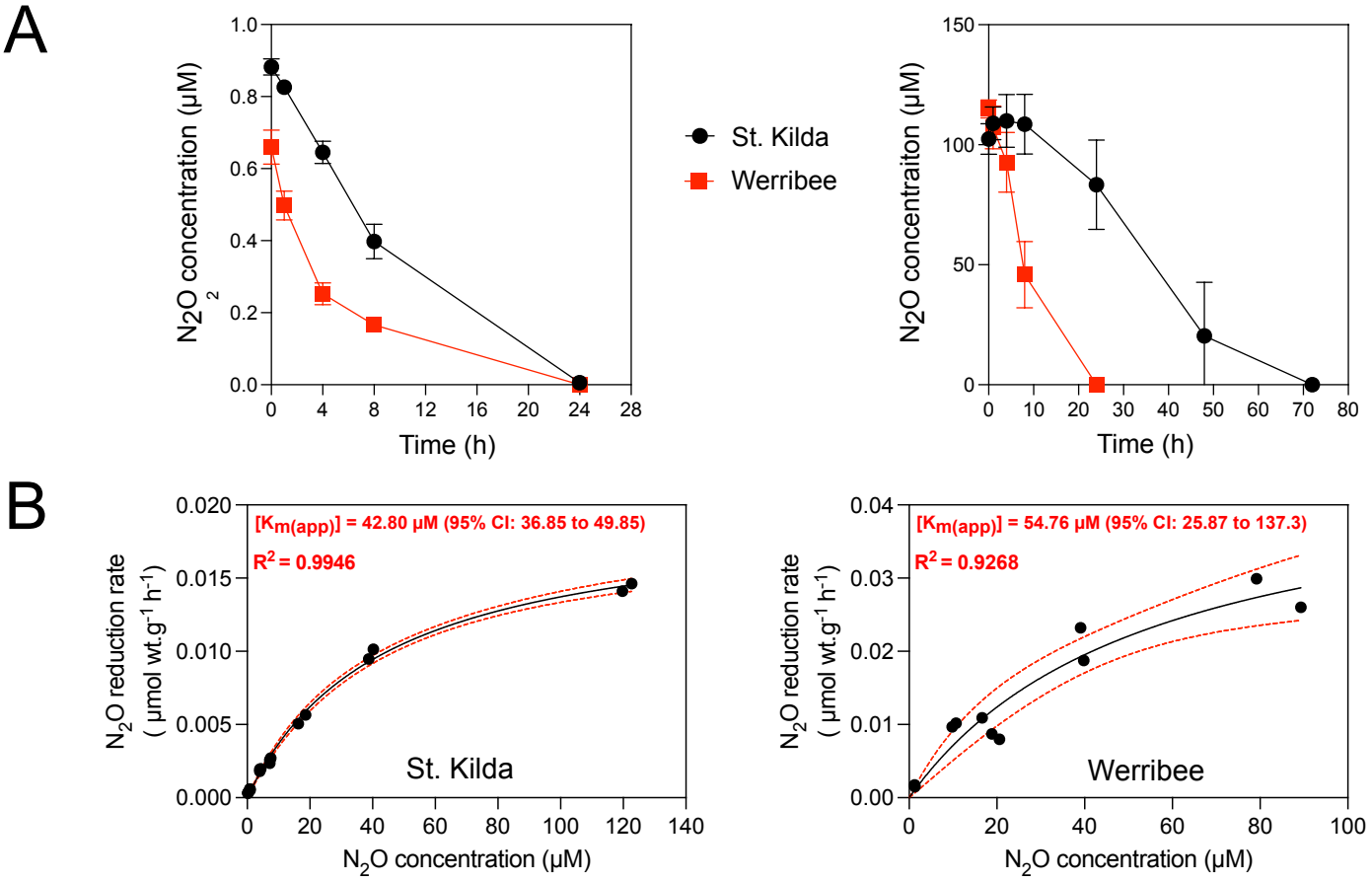
A
B
N_2O concentration (μM)
Time (h)
St. Kilda
Werribee
N_2O concentraiton (μM)
[$K_{m(app)}$] = 42.80 μM (95% CI: 36.85 to 49.85)
R^2 = 0.9946
N_2O reduction rate (μmol wt.g^{-1} h^{-1})
N_2O concentration (μM)
[$K_{m(app)}$] = 54.76 μM (95% CI: 25.87 to 137.3)
R^2 = 0.9268

A

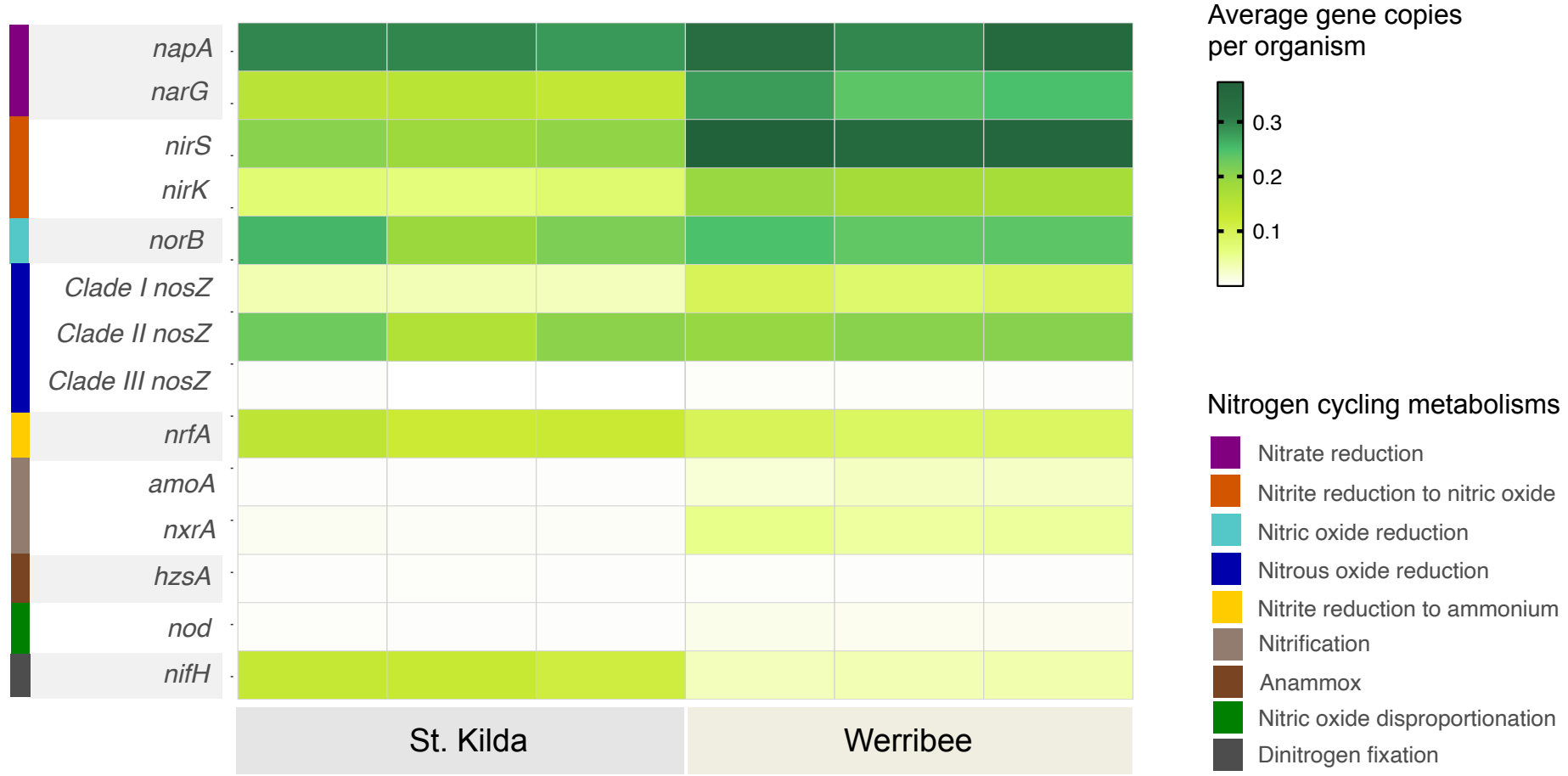

B

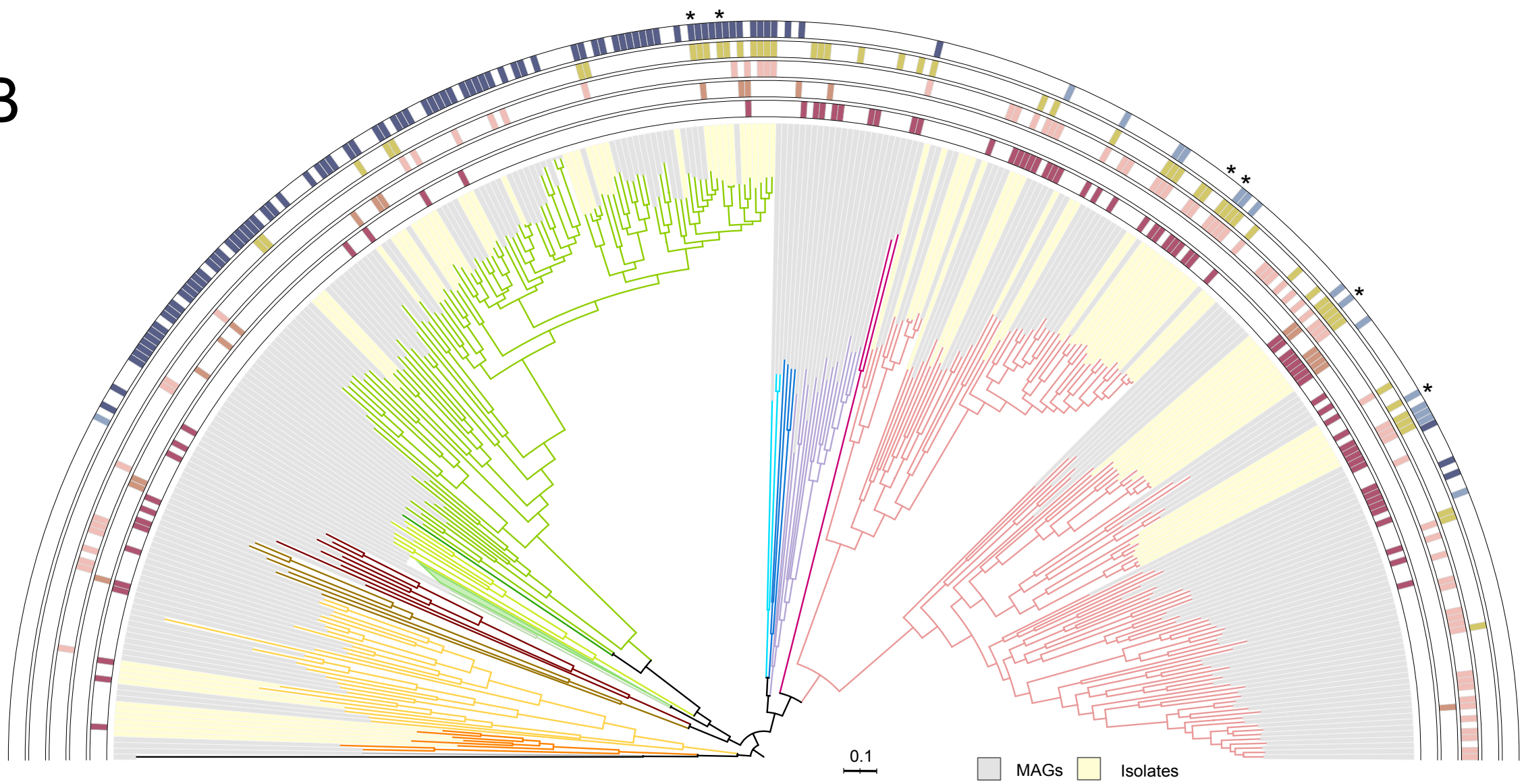

Phylum

- Patescibacteria
- Fusobacteriota
- Bacillota
- Actinomycetota
- Planctomycetota
- Verrucomicrobiota
- Eisenbacteria
- Candidate phyla
- Gemmatimonadota
- Calditrichota
- Bacteroidota
- Myxococcota
- Acidobacteriota
- Desulfobacterota
- Campylobacterota
- Pseudomonadota

Nitrogen metabolising genes

- *napA/narG* (Nitrate reduction)
- *nrfA* (Ammonification)
- *nirK/nirS* (Nitrite reduction)
- *norB* (Nitric oxide reduction)
- Clade I *nosZ* (Nitrous oxide reduction)
- Clade II *nosZ* (Nitrous oxide reduction)

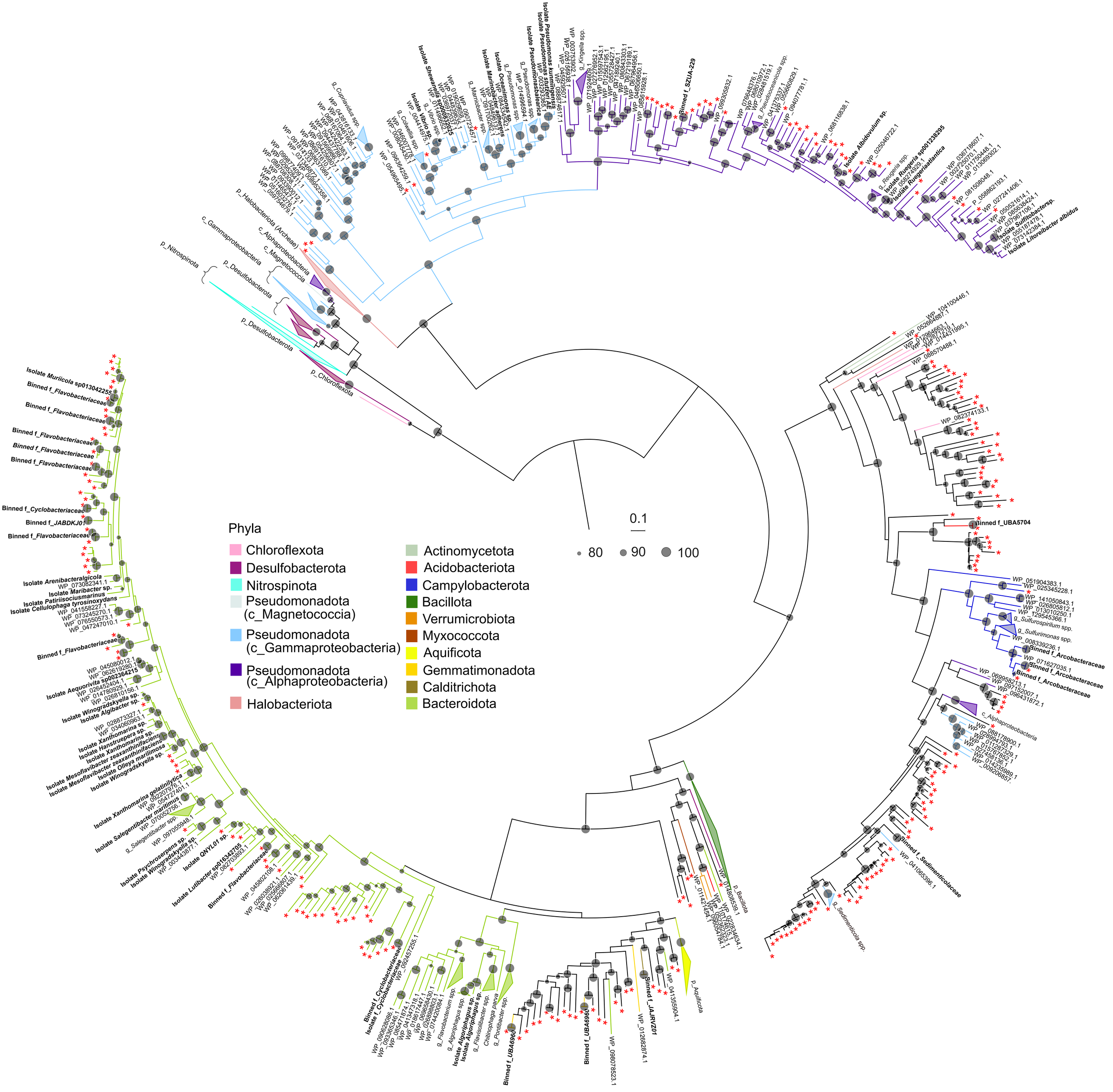

Phyla
Chloroflexota
Desulfobacterota
Nitrospinota
Pseudomonadota (c_Magnetococcia)
Pseudomonadota (c_Gammaproteobacteria)
Pseudomonadota (c_Alphaproteobacteria)
Halobacteriota
Actinomycetota
Acidobacteriota
Campylobacterota
Bacillota
Verrumicrobiota
Myxococcota
Aquificota
Gemmatimonadota
Calditrichota
Bacteroidota
0.1
80
90
100
p_Nitrospinota
p_Desulfobacterota
p_Chloroflexota
c_Gammaproteobacteria
c_Alphaproteobacteria
c_Magnetococcia
p_Halobacteriota (Archeae)
p_Bacillota
p_Aquificota
Binned f_SZUA-229
Binned f_UBA5704
Binned f_Arcobacteraceae
Binned f_Sedimenticolaceae
Binned f_Cyclobacteriaceae
Binned f_Flavobacteriaceae
Isolate Muriicola sp013042255
Isolate Arenibacteralgicola
Isolate Maribacter sp.
Isolate Patiriisociusmarinus
Isolate Cellulophaga tyrosinoxydans
Isolate Aequorivita sp002364215
Isolate Winogradskyella sp.
Isolate Algibacter sp.
Isolate Xanthomarina sp.
Isolate Hanstruepera sp.
Isolate Xanthomarina gelatinilytica
Isolate Salegentibacter maritimus
Isolate Psychroserpens sp.
Isolate Winogradskyella sp.
Isolate QNYL01 sp.
Isolate Lutibacter sp016342705
Isolate Algoriphagus sp.
Isolate Pseudomonas kummingensis
Isolate Pseudomonas stutzeri AE
Isolate Pseudomonasbalearica
Isolate Pseudomonas sp.
Isolate Oceanimonas sp.
Isolate Marinobacter adherens
Isolate Shewanella sp000852025
Isolate Vibrio sp.
Isolate Albidovulum sp.
Isolate Ruegeria sp001238295
Isolate Ruegeriaatlantica
Isolate Sulfitobactersp.
Isolate Litoreibacter albidus
g_Cupriavidus spp.
g_Kingella spp.
g_Pseudomonas spp.
g_Colwellia spp.
g_Marinobacter spp.
g_Reugeria spp.
g_Pseudooceanicola spp.
g_Sulfurospirilum spp.
g_Sulfurimonas spp.
g_Salegentibacter spp.
g_Flavobacterium spp.
g_Algoriphagus spp.
g_Flavisolibacter spp.
Chitinophaga parva
g_Pontibacter spp.
g_Sedimenticola spp.

A

Isolates	$NO_3^- \rightarrow NO_2^-$		$NO_2^- \rightarrow NO$		$NO \rightarrow N_2O$	$N_2O \rightarrow N_2$		
	narG	*napA*	*nirK*	*nirS*	*norB*	Clade I *nosZ*	Clade II *nosZ*	Clade III *nosZ*
Antarctobacter sp.	■		■		■			
Sedimentitalea sp.				■	■			

B

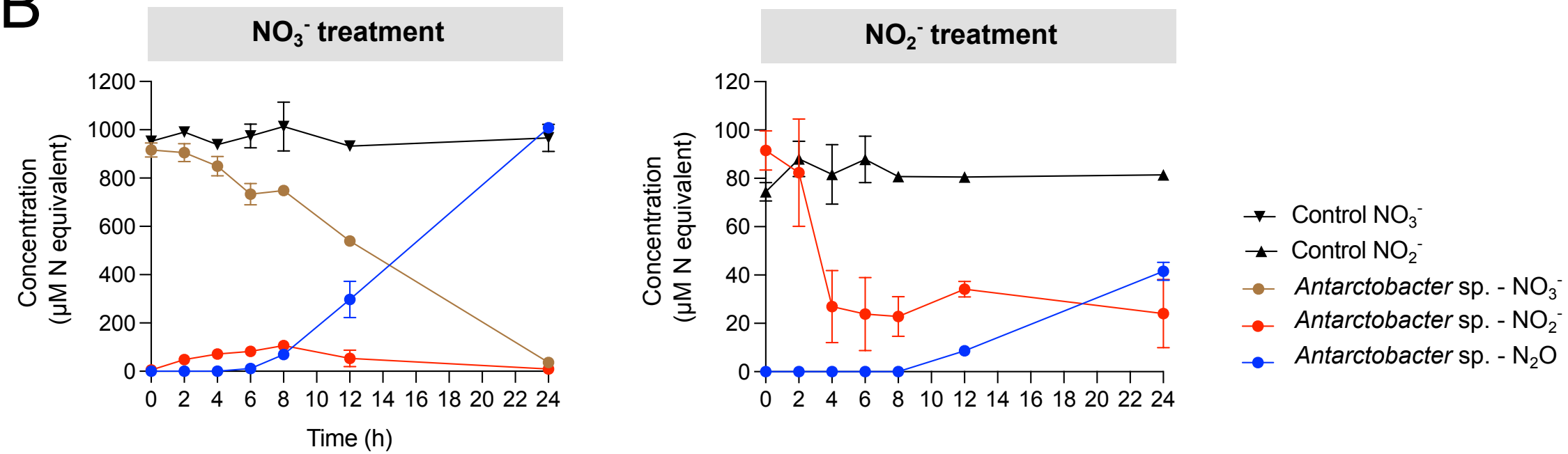

C

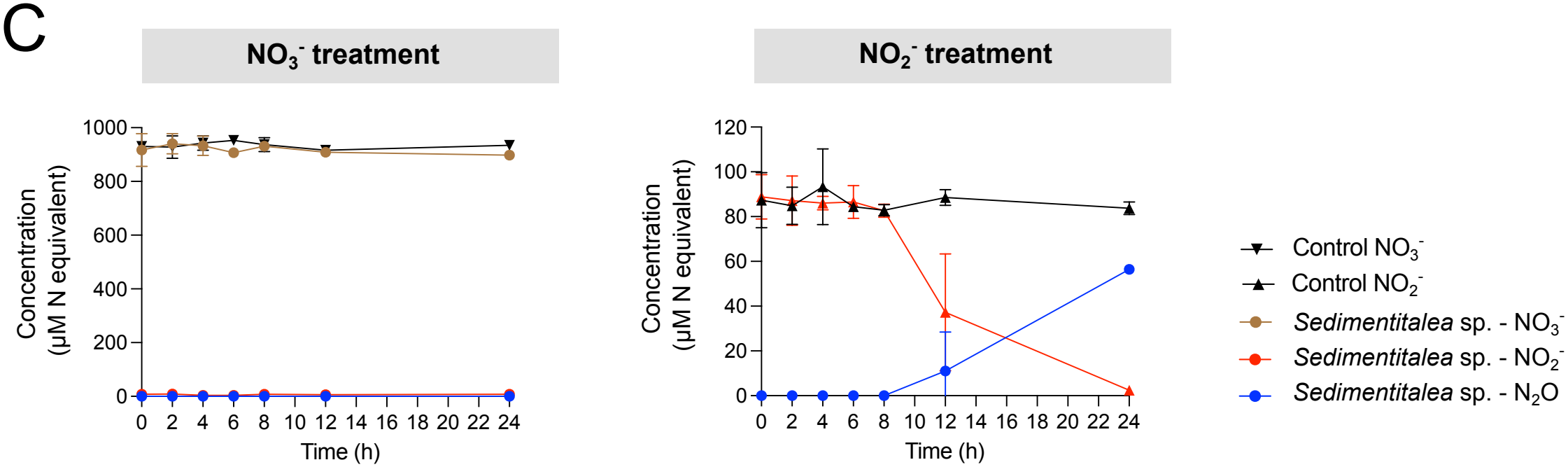

A

Isolates	$NO_3^- \rightarrow NO_2^-$		$NO_2^- \rightarrow NO$		$NO \rightarrow N_2O$	$N_2O \rightarrow N_2$		
	narG	*napA*	*nirK*	*nirS*	*norB*	Clade I *nosZ*	Clade II *nosZ*	Clade III *nosZ*
Olleya marilimosa							■	
Winogradskyella sp.					■		■	
Marinobacter adherens	■				■	■		
Oceanimonas sp.			■		■	■		

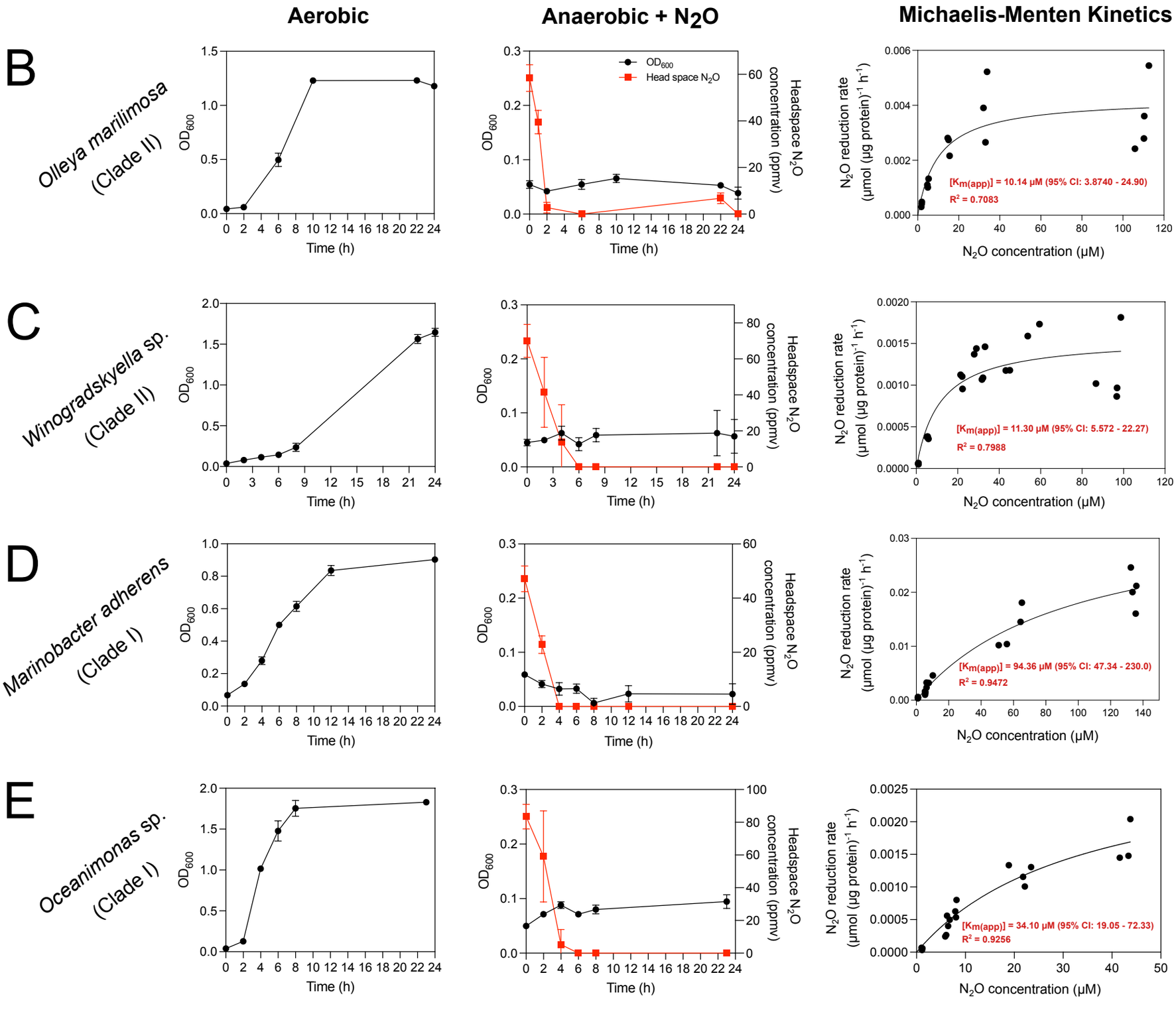

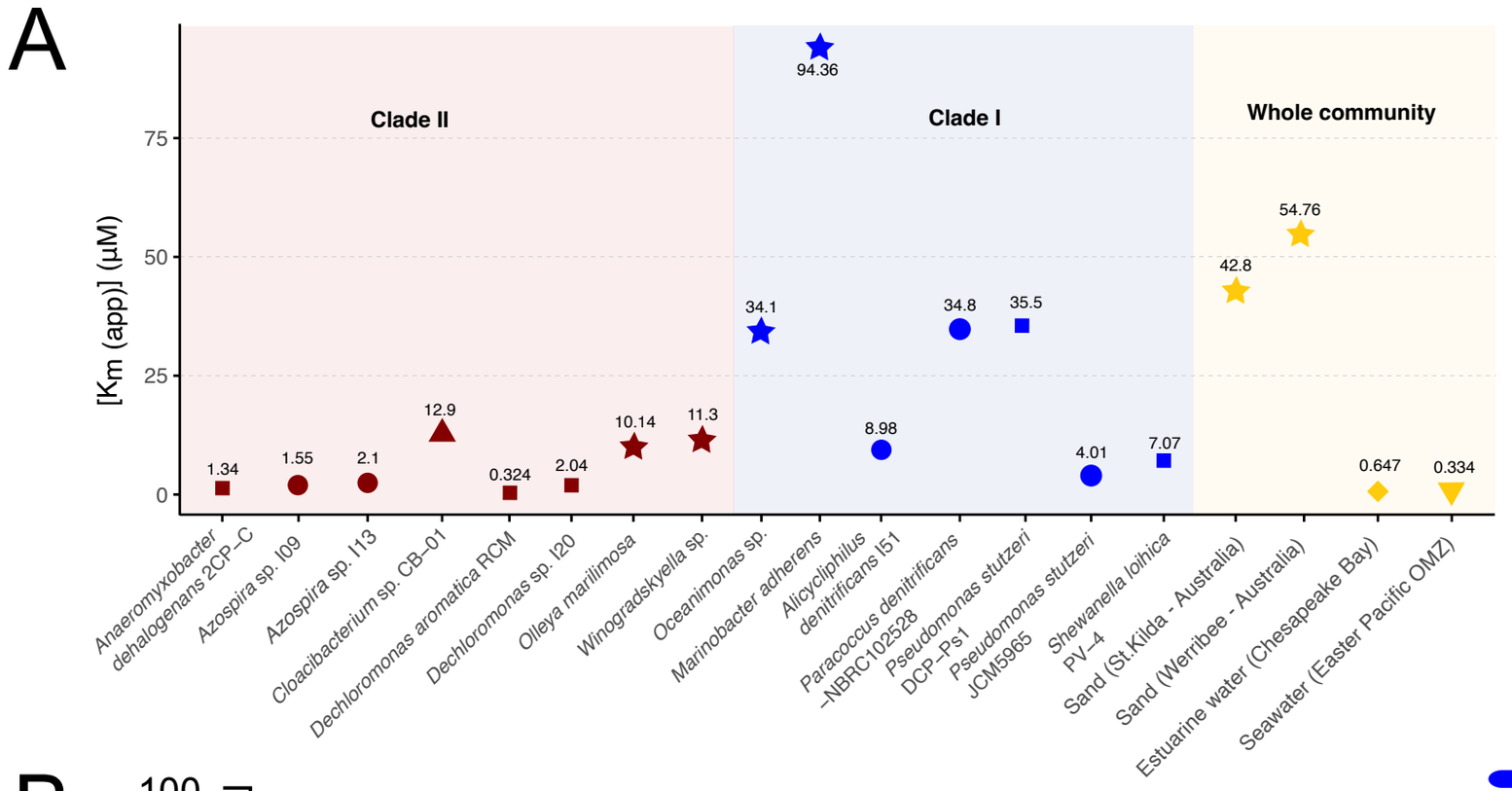
A
Clade II
Clade I
Whole community
[Km (app)] (μM)
75
50
25
0
94.36
54.76
42.8
34.1
34.8
35.5
12.9
10.14
11.3
8.98
4.01
7.07
1.34
1.55
2.1
0.324
2.04
0.647
0.334
Anaeromyxobacter dehalogenans 2CP–C
Azospira sp. I09
Azospira sp. I13
Cloacibacterium sp. CB–01
Dechloromonas aromatica RCM
Dechloromonas sp. I20
Olleya marilimosa
Winogradskyella sp.
Oceanimonas sp.
Marinobacter adherens
Alicycliphilus denitrificans I51
Paracoccus denitrificans –NBRC102528
Pseudomonas stutzeri DCP–Ps1
Pseudomonas stutzeri JCM5965
Shewanella loihica PV–4
Sand (St.Kilda - Australia)
Sand (Werribee - Australia)
Estuarine water (Chesapeake Bay)
Seawater (Easter Pacific OMZ)

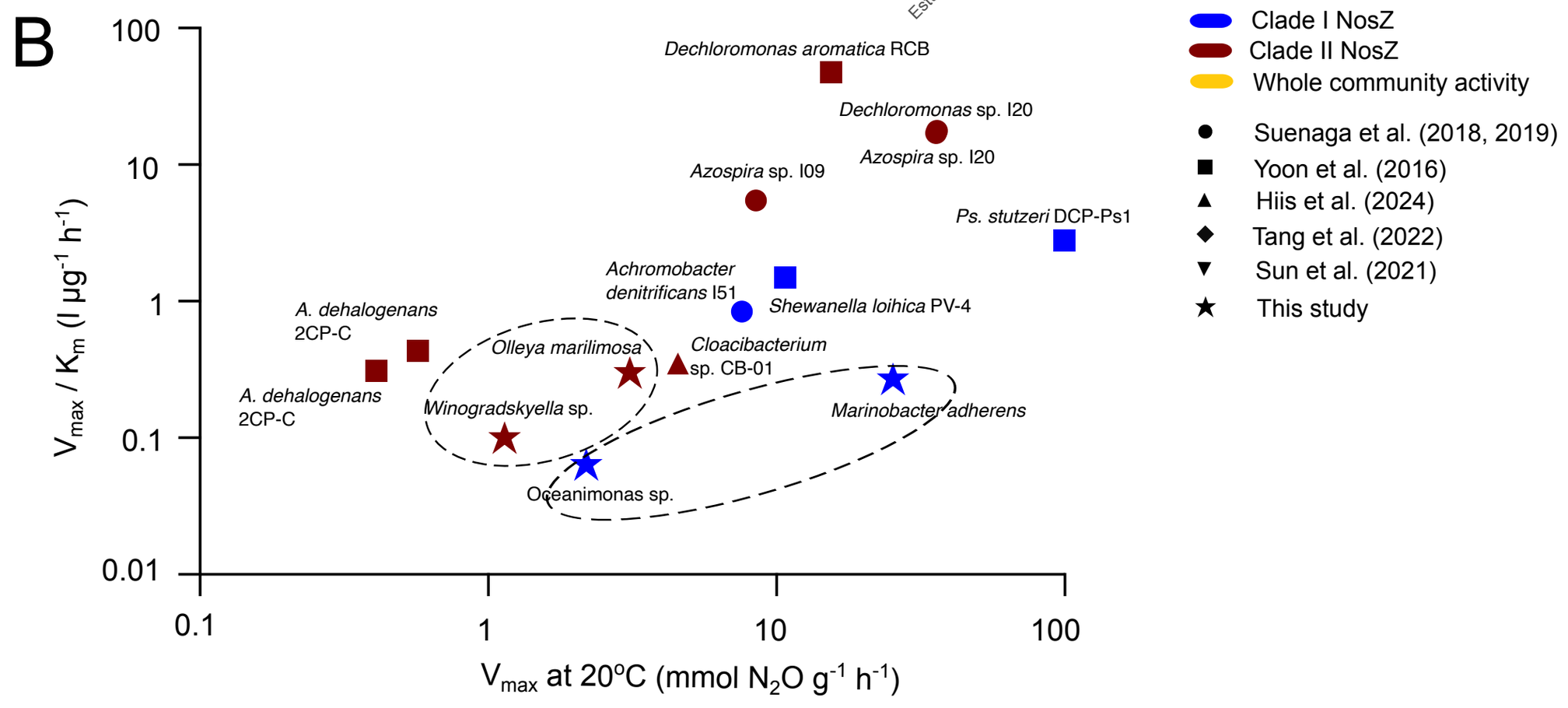
B
100
10
1
0.1
0.01
Vmax / Km (l μg-1 h-1)
0.1
1
10
100
Vmax at 20°C (mmol N2O g-1 h-1)
Dechloromonas aromatica RCB
Dechloromonas sp. I20
Azospira sp. I20
Azospira sp. I09
Ps. stutzeri DCP-Ps1
Achromobacter denitrificans I51
Shewanella loihica PV-4
A. dehalogenans 2CP-C
A. dehalogenans 2CP-C
Olleya marilimosa
Cloacibacterium sp. CB-01
Winogradskyella sp.
Marinobacter adherens
Oceanimonas sp.
Clade I NosZ
Clade II NosZ
Whole community activity
Suenaga et al. (2018, 2019)
Yoon et al. (2016)
Hiis et al. (2024)
Tang et al. (2022)
Sun et al. (2021)
This study